Solar Energy 276 (2024) 112690

Contents lists available at ScienceDirect

Solar Energy

journal homepage: www.elsevier.com/locate/solener

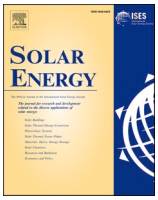

Assessing the light scattering properties of c-Si PV module materials for agrivoltaics: Towards more homogeneous light distribution in crop canopies

Shu-Ngwa Asa'a [a,b,c,*], Giacomo Bizinoto Ferreira Bosco [d], Nikoleta Kyranaki [a,b,c], Arvid van der Heide [a,b,c], Hariharsudan Sivaramakrishnan Radhakrishnan [a,b,c], Jef Poortmans [a,c,e,f], Michael Daenen [a,b,c]

[a] Hasselt University, imo-imomec, Martelarenlaan 42, 3500 Hasselt, Belgium
[b] Imec, imo-imomec, Thor Park 8320, 3600 Genk, Belgium
[c] EnergyVille, imo-imomec, Thor Park 8320, 3600 Genk, Belgium
[d] FOTONIQ, Ampèreweg 16, 2627 BG, Delft, Netherlands
[e] KU Leuven, Department of Electrical Engineering, Kasteelpark Arenberg 10, 3001 Leuven, Belgium
[f] Imec, Kapeldreef 75, 3001 Leuven, Belgium

ARTICLE INFO

Keywords:
Agrivoltaics
Diffuse light
Photovoltaic materials
Haze
Hortiscatter

ABSTRACT

Increasing the diffusivity of transmitted light at crop canopies in agrivoltaic (AV) systems remains a desired objective. This is because diffuse light increases the uniformity of light distribution and penetrates deeper into compact crop canopies thereby enhancing the photosynthesis rate and crop yields. Current approaches in greenhouses and open horticultural systems involve the use of diffusing films, diffuse glass, and light diffusing coatings. While these methods are effective, their combination with photovoltaic (PV) modules in AV greenhouses and other AV farming practices remain relatively unknown. However, little to no work has been done to assess the light scattering properties of the existing PV module structural materials such as the glass, encapsulants and the transparent backsheet. This work therefore investigates the light scattering behaviour of c-Si PV module materials through haze and Hortiscatter measurements. 18 samples with the structural layout of glass/encapsulant/encapsulant/back cover (glass or transparent polymer backsheet), applying different commercial encapsulants, were manufactured and tested experimentally. Light in the photosynthetic spectrum was used in the optical characterization of the samples. Furthermore, the impact of UV degradation on the haziness was also tested and the uniformity of the light distribution was further assessed to obtain the Hortiscatter. The findings indicated that (i) Transparent backsheets increased the light diffusivity. (ii) UV degradation reduced the light scattering of most of the PV materials. (iii) For the haziest transparent backsheet sample, the distribution of the transmitted light increased with the incidence light angle and reduced with increasing wavelength in the visible spectrum (iv) Highest haze and Hortiscatter values of up to 80% and 84% respectively were obtained for a sample with glass/TPO/TPO/transparent backsheet layout. (v) Haze and Hortiscatter values could help in optimising the PV module bill of materials for AV applications.

1. Introduction and background

Agrivoltaics is considered a suitable solution to alleviate land-use competition between photovoltaic installations and agriculture, by enabling the colocation of PV modules and crops on the same land for the simultaneous production of food and green energy. The cumulative

List of abbreviations including units and nomenclature: AOI, Angle of incidence; AV, Agrivoltaics; BRDF, Bidirectional reflectance distribution function; BSDF, Bidirectional scattering distribution function; BTDF, Bidirectional transmittance distribution function; CO_2, Carbon dioxide; c-Si, Crystalline silicon; EVA, Ethylene vinyl acetate; GG, Glass-glass; GTB, Glass-transparent backsheet; HS, Hortiscatter; kWh/m^2, kilowatt-hour per square meter; PAR, Photosynthetically active radiation; POE, Polyolefin elastomer; PV, Photovoltaic; Sr, Steradian; TPO, Thermoplastic polyolefin; UV, Ultraviolet.

* Corresponding author.
E-mail address: shu-ngwa.asaa@uhasselt.be (S.-N. Asa'a).

https://doi.org/10.1016/j.solener.2024.112690
Received 16 April 2024; Received in revised form 5 June 2024; Accepted 9 June 2024
Available online 20 June 2024

global AV installed capacity has exceeded 14 GWp [1] and wafer-based c-Si solar cells account for over 95% of the global market [1]. However, standard c-Si PV modules are opaque in the visible wavelength range which is needed for crop production. Semitransparency can only be achieved by increasing the spaces between the cells in a module coupled with a non-opaque back cover (i.e., glass or transparent polymer backsheet). Nevertheless, the implementation of PV modules above crops inevitably leads to shading which could negatively impact crop growth and crop yields. However, this shading could be (partly) compensated for by increasing the light diffusivity at the crop canopies.

The impact of diffuse light on crop response has been investigated in literature [2]. Crop light use efficiency, water use efficiency and net carbon uptake was higher for cloudy days compared to clear sky days [2]. Plants use diffuse light more efficiently compared to direct light [3]. This is because diffuse light penetrates further into crop canopies resulting in a higher light intensity and photosynthesis capacity on the lower leaves [4]. Diffuse light also results in a more uniform temporal and horizontal light distribution at crop canopies, enhancing crop photosynthesis and crop growth [4]. Short and compact crop canopies induce self-shading [5] which could be compensated for by diffuse light. Light diffusing plastic films with 20% and 29% light diffuseness were tested in Chinese solar greenhouses with tomatoes [6]. The plastic films continuously increased the horizontal and vertical light distribution and enhanced the photosynthesis rate due to lower air and leaf temperature in the summer. Yields of high stem and low stem tomato plants were respectively 5.5% and 12.9% higher under the 29% haze roof compared to the 20% [6]. Studies showed that the middle leaf layers of cucumbers absorbed diffuse light better than direct light which enhanced the photosynthesis rate and yields [7]. Roses grown under diffuse greenhouse glass cover had 5.2% and 6.1% higher number of flowers and fresh weight respectively compared to a reference (clear glass) greenhouse [8]. Tomatoes grown in greenhouses with three levels of light diffuseness (0%, 45% and 71%) showed a 7.2% increase in photosynthesis rate for the 71% scenario [9] for the growing period (April – October). This was attributed to a more uniform horizontal and vertical photosynthetic photon flux density (PPFD; number of photons in the wavelength range 400–700 nm incident per unit time on a given unit surface). Simulations in Dutch horticultural greenhouses with diffuse cover predicted a 5–6% increase in sweet pepper growth [10]. Simulation of tomatoes in greenhouses reported 5.3% and 4.58% increase in carbon uptake and light use efficiency respectively under increasing film diffuseness [11]. Lettuces grown under PV modules with light diffusion films showed high dry weight and high relative growth rate under diffuse light compared to direct light [12]. Light diffusion films underneath semi-transparent PV modules in a greenhouse improved crop yields due to deeper light penetration to the lower leaves and increased total CO_2 assimilation [13]. c-Si PV modules with increased cell spacing and a diffuse cover also increased the photosynthesis rate of blueberries [14].

To understand the impact of diffuse light on the crop photosynthesis rate, an understanding of crops' light response is essential. Fig. 1 shows the photosynthetic light response curve of tomato leaves in the top and middle canopy under non-diffuse (0%) and 71% light diffuseness [9,15]. Based on the crop type, the photosynthesis rate is proportional to the light intensity, and the process increases on the steep part of the curve. The photosynthesis efficiency then plateaus, at which point an increase in light intensity has little effect on the rate of photosynthesis. Beyond this point, an increase in light intensity could lead to a reduction in photosynthesis rate based on the crop type. In Fig. 1, the top leaves showed similar photosynthetic behaviour irrespective of the light diffuseness [9,15]. However, for the tomato leaves in the middle crop canopy, the photosynthetic capacity increased with the light diffuseness [9,15] as indicated by the purple arrow. This is because more light reaches the lower leaves of the crop canopy as the light diffuseness increases, thereby enhancing the overall photosynthesis capacity and the crop growth and yields [15].

Overall, the use of diffuse covers or films has been shown to increase the homogeneity of light distribution at crop canopies, which enhances crop growth. Therefore, application of this concept in AV systems could help alleviate PV-induced shading and enhance agricultural yields. To increase the diffusivity of photosynthetically active radiation (PAR) at the crop canopy in AV systems, very hazy or light diffusing c-Si PV module materials should be used. In current greenhouses and open horticultural systems, diffuse films or covering materials [12,16,17] and coatings [18,19] are currently being used. When combined with PV modules, the impacts of these films on the PV module performance are still relatively unknown. Also, when these coatings are applied on PV modules, their potential thermal impact on the PV module temperature, energy yield and the overall performance of AV systems are not well defined. Furthermore, while the lifetime of PV systems is around 25 years, the lifetime and time-dependent performance of these coatings and films are shorter. Also, spatial light transmission measurements showed that many structured diffusing glasses only result in narrow light scattering [17]. Therefore, materials or solutions which align with

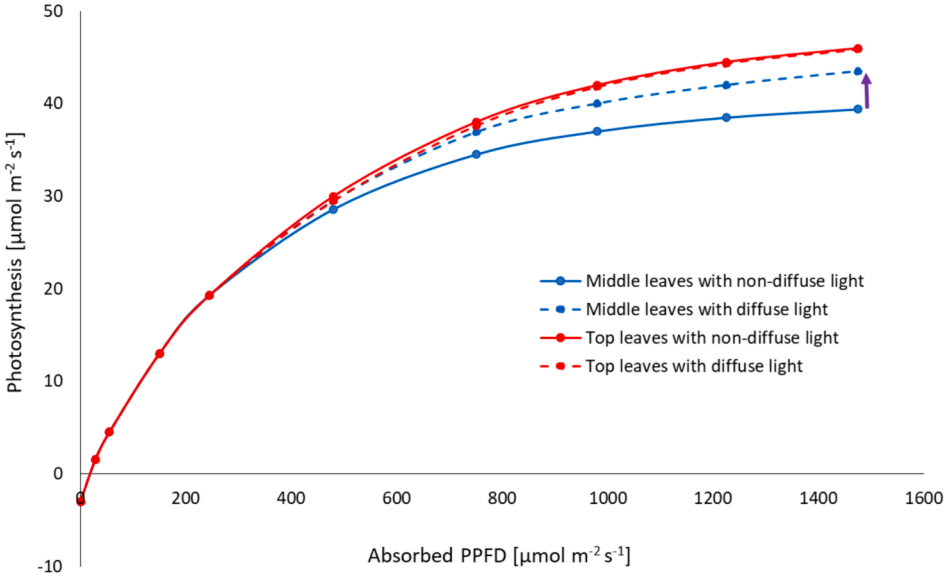

Fig. 1. Photosynthesis response curves of tomato leaves at the top and middle of the canopy under non-diffuse and diffuse (71%) light. Modified from [9,15].

the durability and performance of PV modules while providing increased light diffusivity to crops need to be tested and implemented in AV systems. Little to no work has been done to investigate the PAR scattering properties of c-Si PV module materials such as the glass, encapsulants and transparent backsheet for AV applications.

In this work, we assess the light scattering properties of c-Si PV module materials for AV. In an experimental test of materials, 18 PV material stacks consisting of a front glass, different encapsulants and a rear glass, or transparent backsheet, are manufactured and tested for their haziness according to the ASTM D1003 standard. Each sample stack is representative of the transparent area of a semi-transparent c-Si PV module. The impact of UV degradation on each sample's haziness was also analysed. Next, the incident light angle dependence of the light diffusivity was studied through bidirectional transmittance distribution function measurements for the haziest sample. Lastly, the bidirectional transmittance distribution function measurements were used to calculate the Hortiscatter value in accordance with the NEN 2675+C1:2018 standard. The Hortiscatter represents the extent to which or how uniformly incoming light is diffused by the material. To the best of the authors' knowledge, this is the first work analysing the light scattering and the uniformity of scattered light by such c-Si PV samples for AV applications.

2. Materials and methodology

2.1. PV material sample fabrication and haze measurement

The structural layout of the transparent (inactive) region of a semi-transparent c-Si PV module consists of glass/encapsulant/encapsulant/back cover (glass or transparent backsheet). To investigate the diffusivity of the light incident on such regions, samples of 5x5 cm in size were manufactured using a PV module laminator, applying different commercial encapsulants including ethylene vinyl acetate (EVA), thermoplastic polyolefin (TPO) and polyolefin elastomers (POEs). Fig. 2 shows an example of the sample stack, along with the structural layers.

Each sample stack was laminated based on the optimal lamination conditions defined by the manufacturers and tested with the different encapsulants for both glass-glass (GG) and glass-transparent backsheet (GTB). Table 1 lists the commercial encapsulants, their properties and the layouts of the 18 laminates fabricated in this work.

The haze measurements were carried out using an integrating sphere according to the ASTM D1003 standard and based on the three measurement steps shown in Fig. 3 and similarly described by [20]. In Fig. 3A, the sample is placed at the entrance of the integrating sphere while a white reflecting plate at the rear ensures that the total sample transmitted light (T_t) is recorded by the sensor. In Fig. 3B, the exit of the integrating sphere is opened such that only the light scattered by the sample (T_s) at the entrance is recorded. In Fig. 3C, the light scattered by the equipment (T_e) is measured, which is subtracted from T_s in the calculation of haze as shown in equation (1). The reflected light at the sample surface is neglected in this work. Nevertheless, the reflected light is expected to be very low due to the smooth surfaces and transparent nature of the samples. This study is focused on the diffusivity of light in the PAR spectrum (400–700 nm). The haze measurements were therefore carried out in 5 nm wavelength steps for light in the UV–VIS/NIR spectrum of 375–800 nm.

$$\text{Haze} = \frac{T_s - T_e}{T_t} \tag{1}$$

2.2. Sample UV reliability testing

After the haze measurements, accelerated UV preconditioning tests based on the IEC 61215 standard [21] were carried out to characterize the impact of potential optical degradation on the light scattering properties of the samples. The samples were placed in the UV chamber with the incident light intensity of 100 W/m^2 on the front glass. The Osram Supratec HTC 2000–349 KX10s UV lamps radiate power of 490 W in the wavelength range 315–400 nm (UVA) and 60 W in the range 280–315 nm (UVB). The haze measurements were repeated after the UV reliability tests, and the best (haziest) GG and GTB samples were used for the bidirectional transmittance distribution function measurements.

2.3. Angle dependence measurements of scattered light

Haze measurements give no information on the angular dependence of the scattered light. To determine the angular light profile of the sample in transmission, reflection or both, bidirectional scattering distribution function (BSDF) measurements are needed. BSDF measurements can be separated into reflected and transmitted components respectively known as bidirectional reflectance distribution (BRDF) and bidirectional transmittance distribution (BTDF) measurements. BRDF was first introduced to faithfully characterize diffusely scattered light [22,23]. It was later extended for transmission measurements and known as BTDF [24]. BRDF and BTDF measurements represent how light is angularly reflected or transmitted respectively by a sample for a given wavelength and light angle of incidence (AOI).

2.3.1. BRDF and BTDF measurements

The BRDF is a physical property of a material and defines the pattern of light reflected from the surface of that material to all directions above the surface for all incident angles of light. In the setup for measuring the BRDF, each PV material sample with a surface element dA_i is uniformly irradiated by an incident differential flux (monochromatic light) element dE_i from a direction defined by (θ_i, ϕ_i) and reflected in another direction (θ_r, ϕ_r) per unit solid angle defined by dL_r. The BRDF is calculated as shown in equation (2).

$$BRDF(\theta_i, \varnothing_i, \theta_r, \varnothing_r) = \frac{dL_r(\theta_r, \varnothing_r)}{dE_i(\theta_i, \varnothing_i)} \tag{2}$$

Where θ is the polar angle with respect to the normal of the sample top surface, $\varnothing$ is the azimuth angle within the plane of the sample surface and the subscripts "i" and "r" respectively denote the incident and reflected radiations. The BRDF is also dependent on the wavelength and the polarization of the incident radiation. It has a unit of inverse steradians (sr^{-1}) and takes positive values.

Like BRDF, the BTDF is the ratio of the scattered transmitted radiance dL_t in a specific direction (θ_t, ϕ_t) in the transmittance hemisphere of the sample to the incident differential flux element. The subscript "t" designates the transmitted radiation. The BTDF characterizes the

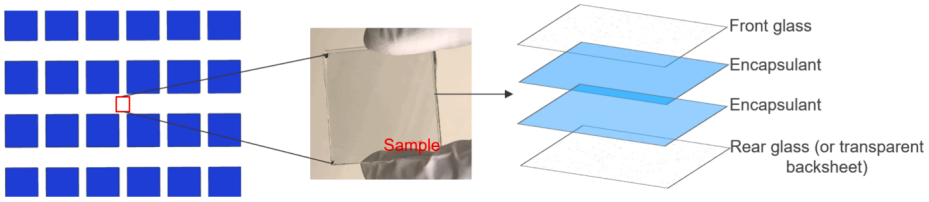

Fig. 2. Schematic view of the structural layers of the samples used in the haze and Hortiscatter measurements. Each sample represents the transparent region of a semi-transparent c-Si PV module.

Table 1
List of different samples with the different encapsulants, their properties and the structural layouts. Each encapsulant was tested for both GG and GTB giving a total of 18 samples.

Sample No.	Encapsulants						Sample layout
	Type	ID	Transmittance (380–1100 nm) [%]	UV-cut off wavelength [nm]	Thickness [mm]	Density [g/cm^3]	
1	TPO	TPO-1	>90	360	0.55	0.88	GG and GTB
2	TPO	TPO-2	>91	–	0.53	0.88	GG and GTB
3	TPO	TPO-3	87	360	0.57	0.89	GG and GTB
4	POE	POE-1	90	–	0.68	0.88	GG and GTB
5	EVA	EVA	> 91	–	0.50	0.95	GG and GTB
6	POE	POE-2	>91	310	0.71	0.88	GG and GTB
7	TPO	TPO-4	>91	–	0.51	0.86	GG and GTB
8	TPO	TPO-5	85	375	0.59	0.88	GG and GTB
9	TPO	TPO-6	89	<300	0.51	0.89	GG and GTB

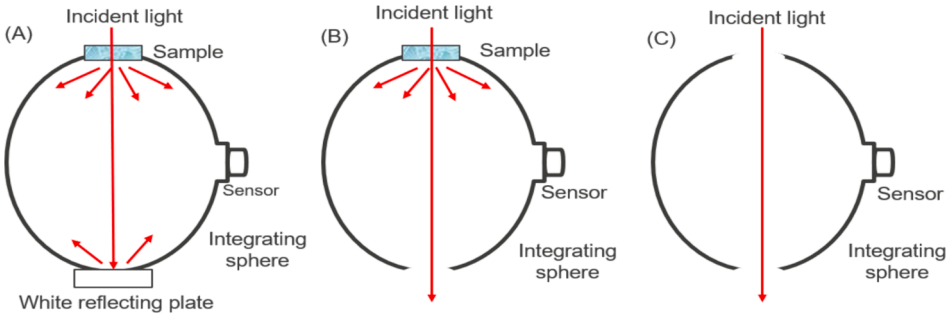

Fig. 3. Illustration of different configurations used to measure the haziness of the PV material samples. (A) Shows the measurement of sample total transmittance, (B) measurement of sample diffuse transmittance and (C) measurement of the equipment diffuse transmittance.

transmitting properties of one point on the PV samples and in a specific direction, with contributions from the entire incident radiation within a given solid angle. Like the BRDF, the BTDF is wavelength dependent and is calculated as shown in equation (3). Fig. 4 shows the geometry of the BRDF and BTDF measurements, indicating the different angles which describe the pattern of incident, reflected and transmitted light. The BTDF also has a unit of sr^{-1} and takes positive numbers. For both BRDF and BTDF measurements, four angles of incidence; 0°, 20°, 40°, and 60° were used.

$$BTDF(\theta_i, \varnothing_i, \theta_t, \varnothing_t) = \frac{dL_t(\theta_t, \varnothing_t)}{dE_i(\theta_i, \varnothing_i)} \tag{3}$$

2.3.2. Description of the Mini-Diff V2 and method to calculate the Hortiscatter

The BTDF and BRDF were obtained via an image-based scattering measurement approach using the Mini-Diff V2 from Synopsys [25]. The Mini-Diff V2 measures the forward scatter and reflection of diffuse materials [26]. The method is based on measuring the lateral distribution of reflected or transmitted luminance using an imaging detector with 640 × 480 pixels to convert the observed point-spread function to a surface's BRDF (or BTDF) at an AOI of 0°. The detector has a dynamic range of five orders of magnitude and allows measurements in the visible range by using, as light sources, monochromatic LEDs with emission centres at 465, 525, and 630 nm. Fig. 5 shows a picture and a schematic of its working principle alongside a description of its most relevant components. The BTDF data collected at 0° AOI is converted to Hortiscatter (HS) following the steps described by the norm NEN 2675+C1 from 2018 where specific data normalization procedures are described [27].

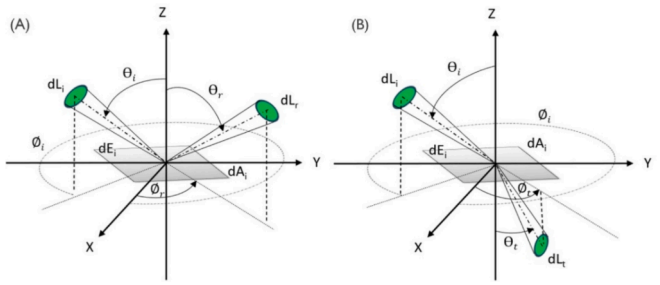

Fig. 4. Geometry of light pathway for (A) BRDF and (B) BTDF measurements.

To calculate the Hortiscatter value, BTDF data generated from a scattering sample is compared to BTDF data generated from the instrument's inherent scattering response. As the samples are isotropic, both BTDFs are averaged out on the azimuth range for a better signal-to-noise ratio. The instrument's response average is $I_R(\theta)$ whereas $I_S(\theta)$ represents the sample's average scattering distribution. The processed transmittance distribution function of the sample (TDF_S) based on the scattering angle for each wavelength is then calculated using equation (4).

$$TDF_S(\theta,\lambda) = \begin{cases} \dfrac{\sum_{\theta=0}^{76} I_R(\theta,\lambda)\dfrac{I_S(\theta=0^\circ,\lambda)}{I_R(\theta=0^\circ,\lambda)}sin\theta}{\sum_{\theta=0}^{75}\sum_{\theta=0}^{76} I_R(\theta,\lambda)\dfrac{I_S(\theta=0^\circ,\lambda)}{I_R(\theta=0^\circ,\lambda)}sin\theta}, if\ \theta = 0^\circ \\ \dfrac{(I_S(\theta,\lambda) - I_R(\theta,\lambda)\dfrac{I_S(\theta=0^\circ,\lambda)}{I_R(\theta=0^\circ,\lambda)})sin\theta}{\sum_{\theta=0}^{75}(I_S(\theta,\lambda) - I_R(\theta,\lambda)\dfrac{I_S(\theta=0^\circ,\lambda)}{I_R(\theta=0^\circ,\lambda)})sin\theta}, otherwise \end{cases} \tag{4}$$

The processed transmittance distribution function of the baseline measurement (TDF_R) for each scattering angle and wavelength is obtained using equation (5).

$$TDF_R(\theta,\lambda) = \begin{cases} \dfrac{\sum_{\theta=0}^{76} I_R(\theta,\lambda)sin\theta}{\sum_{\theta=0}^{75}\sum_{\theta=0}^{76} I_R(\theta,\lambda)sin\theta}, if\ \theta = 0^\circ \\ 0, otherwise \end{cases} \tag{5}$$

Fig. 5. Picture of the Mini-Diff V2 from Synopsys and its schematics. The handheld device has 4 collimated LEDs, one for each AOI, namely 0°, 20°, 40°, and 60°. Three of the LEDs each has a single emission peak at wavelengths of 465 nm, 525 nm, and 630 nm and are focused on the lower part of it. The diffusely reflected light of the probed surface at its bottom is collected and detected by a camera situated on top allowing for BRDF measurements. For transmission measurements, a transmission module with 4 other LEDs allows the camera to capture the BTDF for the same configuration as with the handheld device.

Finally, the Lambertian transmittance distribution function (TDF_L) as a function of the scattering angle is represented by equation (6).

$$TDF_L(\theta) = \frac{\cos(\theta) \times sin(\theta)}{26.85} \tag{6}$$

The next step is to determine the standard deviation, σ_S or σ_R for scattering by the sample or the instrument respectively, from the Lambertian transmittance distribution function as described by equation (7).

$$\sigma_{S,R}(\lambda) = \sqrt{\frac{1}{n} \times \sum_{\theta=0}^{75} \left(\left(TDF_{S,R}(\theta,\lambda) - TDF_L(\theta) \right) - \overline{TDF_{S,R}(\theta,\lambda) - TDF_L(\theta)} \right)^2} \tag{7}$$

where n is the number of scattering angles (n = 76). Finally, the spectral HS is defined by equation (8).

$$HS(\lambda) = \left(1 - \frac{\sigma_S(\lambda)}{\sigma_R(\lambda)} \right)^2 \times 100\% \tag{8}$$

The average HS value from the three wavelengths (465, 525 and 630 nm) is calculated by a linear interpolation between each available wavelength weighted by Planck's law at 3200 K.

3. Theory

3.1. Concepts of haze and Hortiscatter

Fig. 6 illustrates the concepts of both haze and Hortiscatter. Fig. 6A shows the haze as only a measure of how much of the total transmitted light is scattered by more than 2.5°. Haze only describes which portion of the light changes in direction and not about the distribution of the transmitted light. For example, given two materials with the same haze value of 40%, if the first material scatters 40% of the light by 15° and the second material by 35°, the haze method tells us that both materials

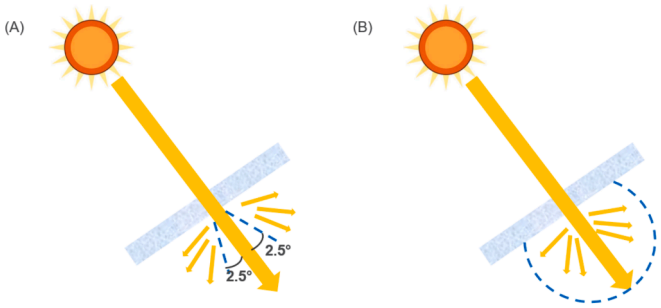

Fig. 6. Illustration of the concepts of haze (A) and Hortiscatter (B) used to characterize the light scattering properties of materials.

create the same light scattering scenarios. This is however not an accurate representation of the light distribution and diffusivity. Also, haze measurements were originally used to assess the level of light diffusion or the transparency of plastics, and not intended for glass [28]. Furthermore, haze is not considered suitable for materials with haze values above 30% [28]. However, a high haze value indicates high light scattering of the sample.

Fig. 6B, illustrates the Hortiscatter which considers all the directions in which the light is scattered. Hortiscatter describes how evenly the incoming light is distributed in all directions. That is, how close the distribution of the transmitted light is to perfect light diffusivity. HS value is expressed as a percentage and ranges between 0% and 100%. A HS value of 100% represents perfect light distribution in all directions according to the Lambertian light scattering, while 0% represents clear glass or a material which does not scatter light. The NEN 2675+C1:2018 standard describes the Hortiscatter of materials and is being used to characterize the light transmittance and scatter of the covering materials, screens and coatings of greenhouses and other horticultural systems [29]. In addition to measuring PAR transmission, the NEN

2675+C1:2018 also involves the UV/VIS/NIR spectrum. Materials with a high Hortiscatter provide better light distribution and contribute to better light utilization of crops as more leaves receive light. This enables the plants to absorb more CO_2 which boosts crop growth, production, and quality [29]. Using materials with a high HS value can therefore increase the uniformity of natural light distribution in crop canopies and ensure uniform and timely crop growth and fruit ripening. This has the potential to reduce the dependence on full-LED lighting in greenhouses for optimizing crop growth and yields. This could contribute to fossil fuel-free and sustainable greenhouse horticultural systems [30]. The NEN 2675+C1:2018 standard requires manufacturers of glasses, coatings and coverings for greenhouses and other open horticultural systems to provide Hortiscatter values. When implemented in AV greenhouses and open AV systems, HS values could therefore enable farmers and growers to choose materials which increase the light distribution in crop canopies. A rule of thumb for tomatoes has been defined: a 1% increase in Hortiscatter can increase yield by 0.3% [31]. Therefore, PV module materials with high HS values can enhance the crop yields in AV systems while producing energy, resulting in higher dual land use productivity.

4. Results and discussion

4.1. Haze and UV reliability testing

The haze values presented here are spectrally averaged (equal weight) for the wavelength range 375–800 nm, which covers the PAR spectrum. Fig. 7 shows the haze values of the 18 samples during the different stages of the UV reliability testing. The results show that the GTB samples (dash lines in Fig. 7) offered higher light diffusivity compared to the GG ones. The backsheet was the main contributor to the haziness. Also, samples with the cross-linking encapsulants (POE and EVA) were less hazy compared to TPO. This is because TPO is a high density polyethylene with shorter or no side chains compared to POE and does not use crosslinking [32]. These features create a more organized and crystalline structure in TPO which enhances its light scattering compared to POE. Also, EVA has no organized stacking of polymer chains (due to the presence of the vinyl acetate group [33] and its crosslinking behavior) which results in a polymer with low light scattering behavior. UV degradation tests with different EVA, TPO and POE materials showed that the EVAs and POEs had similar crystallinity which was lower than that of TPO [32]. While a low degree of crystallinity results in lower haziness, the optical transmittance is expected to be higher [32].

The UV ageing on average reduced the haziness of the GG PV samples. For the GTB samples, there was an observed discoloration of the polymer backsheet. Although no clear trend can be observed, most of the samples showed an initial and continuous decrease in haze with UV exposure, except for TPO-1, TPO-3 and TPO-4 samples which had a strong increase in haze from 40-65 kWh/m^2. In general, the UV degradation of the different encapsulants is dependent on their formulation, i.e., the amount and kind of additive (e.g., stabilizers, antioxidants, curing agents, and adhesion promoters) used [34]. The haziest sample (dash purple line of Fig. 7) was the glass/TPO-4/TPO-4/transparent backsheet sample with a haze value of 81.4% before UV ageing and 80% after UV degradation tests. A haze value of 80% means 80% of the unscattered incident light is scattered by more than 2.5° from the angle at which it strikes the sample surface. It should also be noted that transparent backsheets can vary in their light scattering behavior and not all are expected to have such high haze values. Nevertheless, results from this work show that they increase the scattering of transmitted light compared to a rear glass. The corresponding GG sample with the same TPO encapsulant had the highest haze value for the GG samples, with 42.4% before UV ageing and 34.3% after UV degradation.

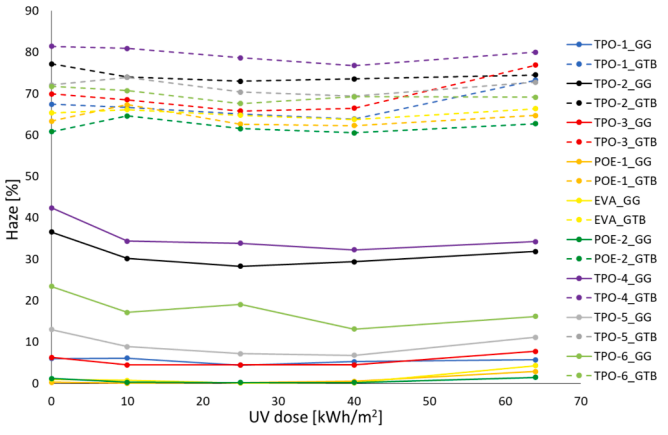

Fig. 7. Haze values for different PV material stacks during the UV reliability tests. The full lines represent the GG samples and dotted lines represent the GTB samples.

Therefore, in AV greenhouse and horticultural systems where high light diffusivity is desired (e.g., crop mutual shading in close planting), semi-transparent c-Si PV modules with a transparent backsheet and TPO encapsulants could be used. Although TPO has a higher cost than EVA, an optimal balance between crop yield and the cost of PV module material can be achieved by using TPO in AV farming practices with high value crops including soft fruits such as berries and specialty greens (e.g., kale, Swiss chard). The potentially higher marketable yields due to enhanced light distribution and photosynthesis rates can override the cost of the TPO. Also, greenhouse crops such as fruit vegetables (eggplants, cucumbers, tomatoes, sweet peppers) with a high plant canopy [7] would also benefit from increased diffuse light as it penetrates deeper into the middle layers enhancing overall canopy photosynthesis rate. Nevertheless, in AV systems, the substructures are the main contributing factor to the high investment costs [1]. Hence the cost of the encapsulant in such applications is not expected to be significant.

By using GTB c-Si PV modules, there are added benefits of reduced mass and associated cost reductions in transportation and installation, better heat dissipation and no alteration to the manufacturing process [35]. Replacing the widely used EVA with TPO encapsulant could also prevent disadvantages such as peroxide-induced crosslinking and the potential formation of corrosive acetic acid which could result in lower reliability of PV modules with EVA [36,37]. The use of EVA in GG modules has also been associated with corrosion and discoloration of PV modules [37]. Nevertheless, GG semi-transparent PV modules continue to dominate the market due to the higher lifespan owing to higher resistance to extreme weather conditions, abrasion, high wind, and dynamic loads [35]. An added benefit to GG modules is their better recyclability [37].

4.2. Polar plots of the BTDF

This work is focused on the scattering of transmitted light for AV applications. Hence, only the results from the BTDF measurements are presented in this paper. To fully characterize the angular distribution of the diffusely transmitted light for different AOIs, the BTDF measurements were carried out for the haziest GG (straight purple line) and GTB (dotted purple line) samples from Fig. 7. The BTDF polar plots for these two samples for 0°, 20°, 40°, and 60° light AOI are presented in Fig. 8. The GG sample (Fig. 8A-D) shows very low diffusivity of the transmitted light, with little to no variation in the light diffusivity with increasing AOI. The transmittance is mostly specular. However, for the hazier GTB sample, the BTDF plots (Fig. 8E-H) show an increase in light scattering with the AOI, indicating an increase in the distribution of transmitted light when the light AOI increases. The BTDF is still non-Lambertian: shows anisotropy which varies with the AOI.

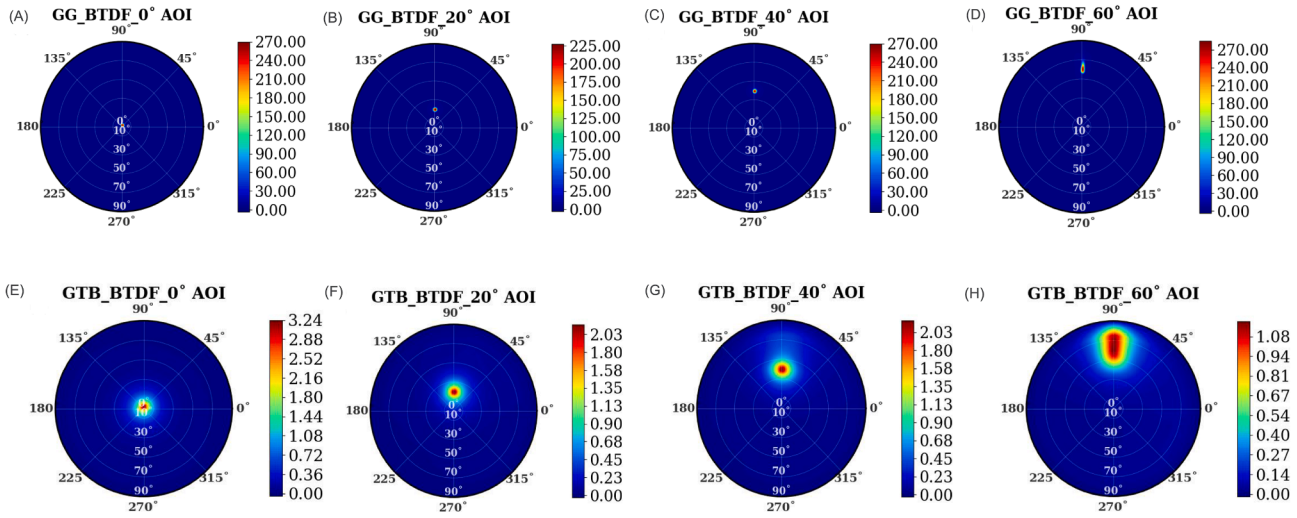

Fig. 8. Polar plots of BTDF (sr^{-1}) for the GG sample (A to D) and the GTB sample (E to H) for four AOIs.

4.3. *Hortiscatter values*

The BTDF plots for the three wavelengths of 465, 525 and 630 nm for the haziest GG and GTB sample are shown in Fig. 9. For the GG sample, (Fig. 9A-C), the BTDF behaviour is similar for all three wavelengths and is mostly specular, while the GTB sample shows an increase in light diffusivity with decreasing wavelength as seen in Fig. 9D-E.

During the measurement by the Mini-Diff at each of the three wavelengths, a distribution function of the sample is obtained for each wavelength and for 0° AOI. Fig. 10 shows the linear plot of the transmittance distribution function for the selected GG (Fig. 10A) and GTB (Fig. 10B) samples at 630 nm wavelength. The distribution function of the GG and GTB sample is plotted against that of a perfectly diffusing material (Lambertian light scattering) and the light distribution of the measurement equipment which is defined as the reference. By averaging the HS at each of the three wavelengths of 465, 525 and 630 nm, HS values of 27.27% and 83.83% were obtained for the GG and GTB sample respectively. A summary of the Haze and HS values for these two samples is plotted in Fig. 11.

Commercially available greenhouse light diffusing materials have a Hortiscatter of about 45% [38], while some medium haze glasses in greenhouses have haze and Hortiscatter values of about 50% and 39% respectively with transmittance of about 91.5% [39], compared to 90.2% and 75.7% transmittance for the haziest GG and GTB samples respectively. Findings from this research therefore suggest that semi-transparent c-Si PV modules with transparent backsheets could have haze and HS values comparable to or higher than those used in commercial greenhouses. It has also been reported that the inner side of some greenhouse glasses have HS values in the range 15–63% [31]. Hence the GG sample with a HS of 27.27% lies in the range of such greenhouse glasses and could therefore be a suitable option in these farming systems.

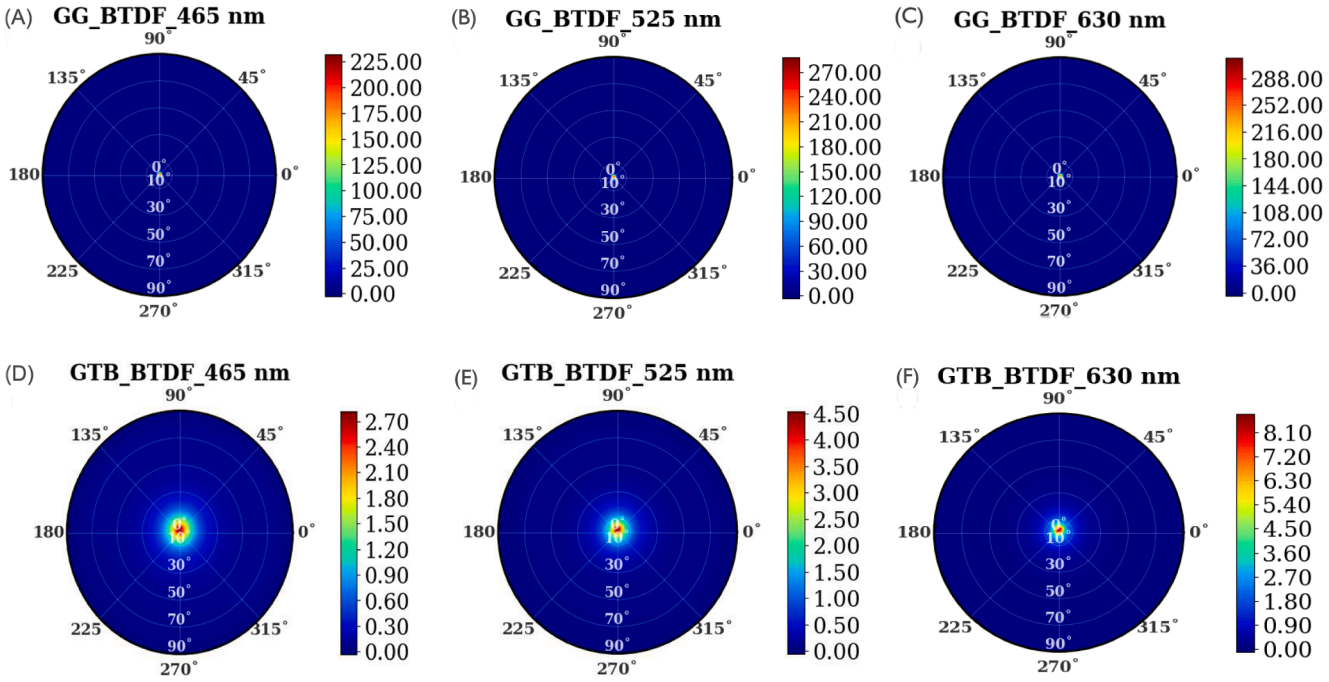

Fig. 9. The BTDF (sr^{-1}) polar plots for the GG (A to C) and GTB (D to F) sample at 0° AOI for 3 wavelengths of 465, 525 and 630 nm. The BTDF data is used to calculate the HS for the two samples based on the NEN 2675+C1:2018 standard.

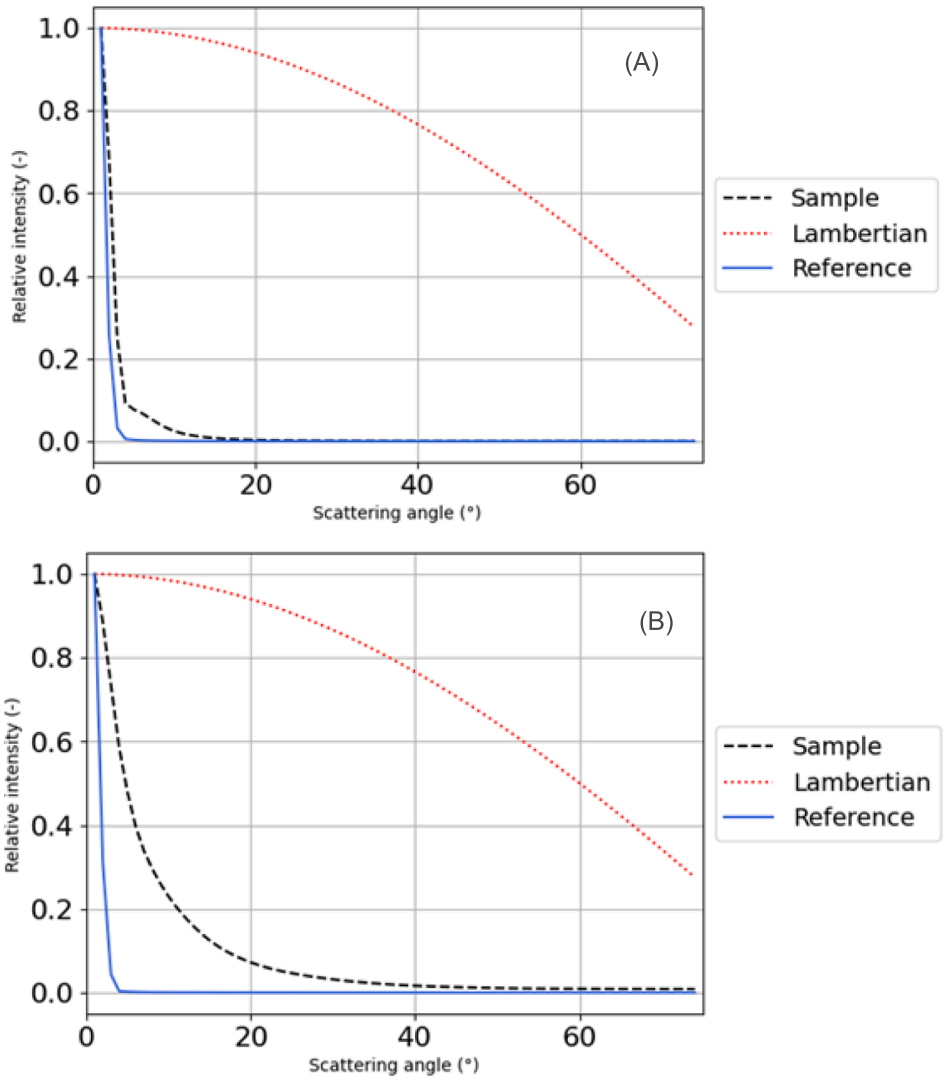

Fig. 10. Linear plot of the distribution function for the (A) GG and (B) GTB samples as measured by the Mini-Diff V2 at 630 nm. The blue curve represents the reference measurement which is the azimuth average transmission distribution function at 0° of incidence of the measurement instrument, $I_R(\theta)$. Similarly, the azimuth average transmission distribution function at 0° of incidence for the GG and GTB samples $I_S(\theta)$ is represented by the black dashed line as measured at 630 nm. The dotted line in red represents the cosine distribution of a Lambertian emitter. (For interpretation of the references to colour in this figure legend, the reader is referred to the web version of this article.)

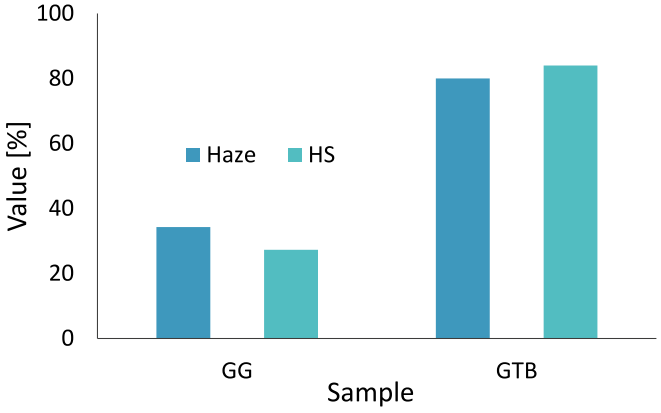

Fig. 11. Summary of the highest haze and HS values for the best GG and GTB samples in this work. The encapsulant in each sample is TPO based, represented as sample 7 in Table 1.

From this work, there is an apparent trade-off in transmittance and haziness. While the GTB has a higher haze and Hortiscatter than the GG sample, its total transmittance is about 16.1% lower than that of the GG. This reduction in light intensity could have a negative impact on the crop growth and yields. Hence, the choice and suitability of GG or GTB is also dependent on many factors such as the crop light requirements, crop canopy, weather, and location. For some shade tolerant crops, the reduction in light intensity might have little to no negative impact on the plant growth and yield due to their lower light requirements and ability to adapt to lower light intensity [40]. The crop canopy type would also influence the choice of GG or GTB materials. For example, cucumbers have a high leaf area index resulting in higher light interception of the upper leaves and lower light reaching the lower leaves [7]. Hence, high light diffuseness with GTB would be desired in such farming systems. Nevertheless, the total light loss must be assessed for an optimal photosynthesis rate. The choice of a high light transmitting, or hazy material is also dependent on the season, as photosynthesis of the upper leaves is far from light saturation in the winter [4] and hence, increased light diffuseness will have a lower effect on the photosynthesis [41]. However, in summer periods with high light intensities, high light

diffuseness is desired as the photosynthesis rate of the upper canopy leaves is close to saturation while that of the lower leaves is unsaturated [41]. It was reported that diffuse light is less beneficial in winter compared to late spring, summer, and early autumn where most of the light is direct [7]. Therefore, in regions characterized by frequent low light intensities and cloudy days, high haze PV materials might not be beneficial for crop growth while crops in regions with frequent sunny days or high light intensities might achieve higher photosynthesis rate under high light diffuseness. Crops in semi-arid and hot regions with high sun intensities might also benefit from high light diffuseness [42] compared to high transmittance due to lower plant stress owing to the lower air and leaf temperature [6,7]. Cucumbers in a greenhouse with diffuse glass had higher productivity compared to clear glass in Saudi Arabia [43]. The water consumption was also 16% lower while electricity consumption was lower (due to a lower cooling load) under the diffuse light. Therefore, the choice of GG or GTB material for AV greenhouses and open AV systems must be optimized and implemented based on crop needs, crop type and could vary from one location to another. It was suggested that materials with a minimum haze of 50% should be used for greenhouses while transmittance (hemispherical) should be above 82% in winter when light is the limiting factor [7]. Nevertheless, at the PV module level, optimizations through higher inter-cell spacings and the use of anti-reflective (AR) coatings could further enhance the intensity of transmitted light for GTB modules.

5. Conclusion and outlook

The installation of PV modules above crops in AV systems inherently leads to shading which could be (partly) compensated for by increasing the light diffusivity at the crop canopy. This is because plants use diffuse light more efficiently compared to direct light as diffuse light results in a more uniform horizontal and temporal light distribution and enhances the photosynthesis rate. In this work, the diffusivity of light in the PAR range by semi-transparent c-Si PV module materials is investigated. Based on an experimental material characterization, different samples consisting of different commercial encapsulants (EVA, TPO, POE) coupled with a transparent front glass and back cover (glass or transparent backsheet) were manufactured, and the haziness analysed. The samples with transparent backsheet showed higher light scattering than the GG samples while the non-cross linking encapsulant (TPO) improved the haziness compared to EVA and POE. Furthermore, the light diffusivity of most samples generally reduced with UV degradation.

The Hortiscatter for the haziest GG and GTB samples was also obtained based on the NEN 2675+C1:2018 standard. The BTDF measurements for the GG sample showed very low angular distribution while the hazier GTB sample showed increasing scattering of the transmitted light as the AOI increased from 0° to 60°. The GTB sample also showed a reduction in the scattering of transmitted light with increasing wavelength in the visible range. Finally, the GTB sample with a haze value of 80% (after UV ageing) had a Hortiscatter of 84%, while the GG sample had haze and Hortiscatter values of 34.3% and 27.3% respectively.

The results from this work indicate that semi-transparent c-Si modules with a TPO encapsulant and a transparent backsheet could be suitable for increasing the light diffusivity in AV greenhouses and open horticultural systems. TPO could therefore be a suitable alternative to EVA for increasing the light diffusivity in AV systems while preventing the potential formation of corrosive acetic acid associated with the potential degradation of PV modules with EVA.

Nevertheless, there was an observed trade-off between haze (and Hortiscatter) and the total transmittance. Therefore, the choice of GG or GTB modules for AV systems will also be influenced by the crop light requirements, the crop canopy structure, location, and the season. Other PV module design optimizations such as lower cell densities and the use of AR coatings could also enhance the total light transmittance in applications with GTB PV modules.

While the impact of diffuse light on the crop light distribution and growth is well known, an in-depth understanding of the impact of high light-scattering PV materials on the PV energy yield is relatively unknown. Research via simulations or experimental measurements on the energy yield of PV modules with different light-diffusing materials is needed to fully understand their impact on PV energy yield. Nevertheless, the haze and Hortiscatter data from this work could be invaluable input for the modelling and simulation of irradiance distribution at crop canopies and for predicting potential increase in the crop yields in AV systems. Finally, the haze and Hortiscatter values can provide desired guidelines for PV module and PV material developers, AV system developers and farmers in optimising the bill of materials of PV modules for AV greenhouses and open AV systems. Through this, the light distribution in crop canopies can be enhanced, and crop yields and quality increased.

Funding

This work is funded by the European Union through the Horizon Europe Research and Innovation programme SYMBIOSYST under grant agreement no. 101096352. This work is also funded by the Fonds Wetenschappelijk Onderzoek – Vlaanderen (FWO) through the SB PhD Fellowship under grant number 1SHF024N. The funders had no role in the study design, data collection and analysis, decision to publish, or preparation of this work.

CRediT authorship contribution statement

Shu-Ngwa Asa'a: Writing – review & editing, Writing – original draft, Visualization, Methodology, Investigation, Formal analysis, Conceptualization. **Giacomo Bizinoto Ferreira Bosco:** Writing – review & editing, Visualization, Resources, Methodology, Investigation, Formal analysis. **Nikoleta Kyranaki:** Writing – review & editing. **Arvid van der Heide:** Writing – review & editing, Supervision. **Hariharsudan Sivaramakrishnan Radhakrishnan:** Writing – review & editing, Supervision. **Jef Poortmans:** Writing – review & editing, Supervision. **Michael Daenen:** Writing – review & editing, Supervision.

Declaration of competing interest

The authors declare that they have no known competing financial interests or personal relationships that could have appeared to influence the work reported in this paper.

References

[1] M. Trommsdorff et al., Agrivoltaics: opportunities for agri-culture and the energy transition, Accessed: Apr. 27, 2023. [Online]. Available: https://www.ise.fraunhofer.de/content/dam/ise/en/documents/publications/studies/APV-Guideline.pdf.
[2] M. Zhang, et al., Effects of cloudiness change on net ecosystem exchange, light use efficiency, and water use efficiency in typical ecosystems of China, Agric. For. Meteorol. 151 (7) (Jul. 2011) 803–816, https://doi.org/10.1016/J.AGRFORMET.2011.01.011.
[3] L. Gu, et al., Response of a deciduous forest to the Mount Pinatubo eruption: enhanced photosynthesis, Science 299 (5615) (Mar. 2003) 2035–2038, https://doi.org/10.1126/SCIENCE.1078366.
[4] T. Li, Q. Yang, Advantages of diffuse light for horticultural production and perspectives for further research, Front. Plant Sci. 6 (september) (2015), https://doi.org/10.3389/fpls.2015.00704. Frontiers Research Foundation.
[5] D.S. Falster, M. Westoby, Leaf size and angle vary widely across species: what consequences for light interception? New Phytol. 158 (3) (Jun. 2003) 509–525, https://doi.org/10.1046/J.1469-8137.2003.00765.X.
[6] L. Zheng, et al., Effects of diffuse light on microclimate of solar greenhouse, and photosynthesis and yield of greenhouse-grown tomatoes, HortSci. 55 (10) (Oct. 2020) 1605–1613, https://doi.org/10.21273/HORTSCI15241-20.
[7] S. Hemming, T. Dueck, J. Janse, F. Van Noort, The effect of diffuse light on crops, Acta Hortic. vol. 801 (PART 2) (2008) 1293–1300, https://doi.org/10.17660/ACTAHORTIC.2008.801.158.
[8] N. García Victoria, F.L.K. Kempkes, P. Van Weel, C. Stanghellini, T.A. Dueck, M. Bruins, Effect of a Diffuse Glass Greenhouse Cover on Rose Production and Quality.

[9] T. Li, E. Heuvelink, T.A. Dueck, J. Janse, G. Gort, L.F.M. Marcelis, Enhancement of crop photosynthesis by diffuse light: quantifying the contributing factors, Ann. Bot. 114 (1) (Jul. 2014) 145–156, https://doi.org/10.1093/AOB/MCU071.

[10] S. Hemming, N. Van Der Braak, T. Dueck, R. Jongschaap, N. Marissen, Filtering natural light by the greenhouse covering using model simulations - More production and better plant quality by diffuse light? Acta Hortic. 711 (2006) 105–110, https://doi.org/10.17660/ACTAHORTIC.2006.711.10.

[11] J. Shin, et al., Evaluation of the light profile and carbon assimilation of tomato plants in greenhouses with respect to film diffuseness and regional solar radiation using ray-tracing simulation, Agric. For. Meteorol. 296 (Jan. 2021) 108219, https://doi.org/10.1016/J.AGRFORMET.2020.108219.

[12] A. Tani, S. Shiina, K. Nakashima, M. Hayashi, Improvement in lettuce growth by light diffusion under solar panels, J. Agric. Meteorol. 70 (3) (Sep. 2014) 139–149, https://doi.org/10.2480/agrmet.D-14-00005.

[13] S. Gorjian, et al., Progress and challenges of crop production and electricity generation in agrivoltaic systems using semi-transparent photovoltaic technology, Renew. Sustain. Energy Rev. 158 (2022), https://doi.org/10.1016/j.rser.2022.112126. Elsevier Ltd.

[14] O.A. Katsikogiannis, H. Ziar, O. Isabella, Integration of bifacial photovoltaics in agrivoltaic systems: a synergistic design approach, Appl. Energy 309 (Mar. 2022), https://doi.org/10.1016/j.apenergy.2021.118475.

[15] T. Dueck, J. Janse, F. Kempkes, T. Li, A. Elings, S. Hemming, "Diffuse light in tomato," 2012, Accessed: Jun. 05, 2024. [Online]. Available: www.glastuinbouw.wur.nl.

[16] M.de.los.Á. Moreno-Teruel, F.D. Molina-Aiz, A. Peña-Fernández, A. López-Martínez, D.L. Valera-Martínez, The effect of diffuse film covers on microclimate and growth and production of tomato (Solanum lycopersicum l.) in a mediterranean greenhouse, Agronomy 11 (5) (2021) 860, https://doi.org/10.3390/AGRONOMY11050860/S1.

[17] S. Hemming, V. Mohammadkhani, J. Van Ruijven, Material technology of diffuse greenhouse covering materials - influence on light transmission, light scattering and light spectrum, Acta Hortic. 1037 (2014) 883–896, https://doi.org/10.17660/ACTAHORTIC.2014.1037.118.

[18] "Removable coatings for a better greenhouse climate. : ReduSystems." Accessed: Jan. 15, 2024. [Online]. Available: https://www.redusystems.com/en/products.

[19] "PAR+ by FOTONIQ." Accessed: Jan. 15, 2024. [Online]. Available: https://www.fotoniq.com/.

[20] "Haze Value Measurement using a UV-Visible Spectrophotometer | JASCO." Accessed: Jan. 23, 2024. [Online]. Available: https://jascoinc.com/applications/haze-measurement-uvvisible-spectrophotometer/.

[21] M. D. Kempe, "Accelerated UV Test and Evaluation Methods for Encapsulants of Photovoltaic Modules (Presentation)." Accessed: Mar. 28, 2024. [Online]. Available: https://www.nrel.gov/docs/fy08osti/43309.pdf.

[22] F.E. Nicodemus, Directional reflectance and emissivity of an opaque surface, Appl. Opt. 4 (7) (Jul. 1965) 767, https://doi.org/10.1364/AO.4.000767.

[23] F.E. Nicodemus, J.C. Richmond, J.J. Hsia, W.E. Ginsberg, T. Limperis, "Geometrical Considerations and Nonmenclature for Reflectance", doi: 10.6028/NBS.MONO.160.

[24] F.O. Bartell, E.L. Dereniak, W.L. Wolfe, F.O. Bartell, E.L. Dereniak, W.L. Wolfe, The Theory and measurement of bidirectional reflectance distribution function (Brdf) and bidirectional transmittance distribution function (BTDF), SPIE 257 (Mar. 1981) 154–160, https://doi.org/10.1117/12.959611.

[25] M.E. Becker, "Measurement and Evaluation of Display Scattering." [Online]. Available: www.display-metrology.com.

[26] "Measuring diffuse light: light diffusion and Hortiscatter - WUR." Accessed: Feb. 12, 2024. [Online]. Available: https://www.wur.nl/en/research-results/research-institutes/plant-research/greenhouse-horticulture/research-themes/energyclimate/lightlab-unique-measurement-facilities-for-greenhouse-cover-and-screen-materials/measuring-diffuse-light-light-diffusion-and-hortiscatter.htm.

[27] "NEN 2675+C1:2018."Horticultural Greenhouses - Determination of the Optical Properties of Greenhouse Cover and Screen Materials," Nederlands Normalisatie Insitute. Accessed: Feb. 12, 2024. [Online]. Available: https://www.nen.nl/nen-2675-c1-2018-en-251294.

[28] "Haze replaced by Hortiscatter provides more information about light distribution : ReduSystems." Accessed: Feb. 13, 2024. [Online]. Available: https://www.redusystems.com/nl/artikelen/haze-vervangen-door-hortiscatter-geeft-meer-informatie-over-lichtverdeling.

[29] "launch of two new NEN standards for diffuse glass." Accessed: Feb. 12, 2024. [Online]. Available: https://www.hortivation.nl/en/innovation/nen/.

[30] "GREENHOUSE2030: Sustainable production for the future - WUR." Accessed: Feb. 12, 2024. [Online]. Available: https://www.wur.nl/en/research-results/research-institutes/plant-research/greenhouse-horticulture/show-greenhouse/greenhouse2030.htm.

[31] "'Horticatter as a defining factor in higher yields.'" Accessed: Mar. 29, 2024. [Online]. Available: https://www.mmjdaily.com/article/9360092/hortiscatter-as-a-defining-factor-in-higher-yields/.

[32] V. Fiandra, L. Sannino, C. Andreozzi, G. Flaminio, M. Pellegrino, New PV encapsulants: assessment of change in optical and thermal properties and chemical degradation after UV aging, Polym. Degrad. Stab. 220 (Feb. 2024) 110643, https://doi.org/10.1016/J.POLYMDEGRADSTAB.2023.110643.

[33] B.K. Sharma, U. Desai, A. Singh, A. Singh, Effect of vinyl acetate content on the photovoltaic-encapsulation performance of ethylene vinyl acetate under accelerated ultra-violet aging, J. Appl. Polym. Sci. 137 (2) (2020), https://doi.org/10.1002/APP.48268.

[34] S. Uličná, A. Sinha, D.C. Miller, B.M. Habersberger, L.T. Schelhas, M. Owen-Bellini, PV encapsulant formulations and stress test conditions influence dominant degradation mechanisms, Sol. Energy Mater. Sol. Cells 255 (Jun. 2023) 112319, https://doi.org/10.1016/J.SOLMAT.2023.112319.

[35] "JinkoSolar: Transparent backsheet vs dual glass—- Advantages and disadvantages - PV Tech." Accessed: Feb. 13, 2024. [Online]. Available: https://www.pv-tech.org/industry-updates/jinkosolar-transparent-backsheet-vs-dual-glass-advantages-and-disadvantages/.

[36] G. Oreski, et al., Properties and degradation behaviour of polyolefin encapsulants for photovoltaic modules, Prog. Photovolt. Res. Appl. 28 (12) (Dec. 2020) 1277–1288, https://doi.org/10.1002/pip.3323.

[37] A. Sinha, et al., Glass/glass photovoltaic module reliability and degradation: a review, J. Phys. D Appl. Phys. 54 (41) (2021) Aug, https://doi.org/10.1088/1361-6463/AC1462.

[38] H. Silke, "Smart materials for greenhouses," in *Agricultural Film*, Barcelona, Nov. 2019.

[39] "Diffused Greenhouse Glass." Accessed: Mar. 29, 2024. [Online]. Available: https://www.dyglassco.com/products/diffused-greenhouse-glass.

[40] I. Ruberti, G. Sessa, A. Ciolfi, M. Possenti, M. Carabelli, G. Morelli, Plant adaptation to dynamically changing environment: the shade avoidance response, Biotechnol. Adv. 30 (5) (Sep. 2012) 1047–1058, https://doi.org/10.1016/J.BIOTECHADV.2011.08.014.

[41] V. Sarlikioti, P.H.B. De Visser, G.H. Buck-Sorlin, L.F.M. Marcelis, How plant architecture affects light absorption and photosynthesis in tomato: towards an ideotype for plant architecture using a functional–structural plant model, Ann. Bot. 108 (6) (Oct. 2011) 1065, https://doi.org/10.1093/AOB/MCR221.

[42] "Enhance Greenhouse Production With Diffuse Light - Greenhouse Grower." Accessed: Jun. 04, 2024. [Online]. Available: https://www.greenhousegrower.com/production/crop-inputs/enhance-greenhouse-production-with-diffuse-light-2/.

[43] A. Alharbi, et al., Effect of clear and defuse glass covering materials on fruit yield and energy efficiency of greenhouse cucumber grown in hot climate, Acta Scientiarum Polonorum, Hortorum Cultus 20 (3) (Jun. 2021) 37–44, https://doi.org/10.24326/ASPHC.2021.3.4.